



H-Infinity VF Controller-Based Three-Phase Voltage Source Parallel Autonomous Grid

Erum Pathan^{1*}, Mubashir Hayat Khan², Haider Arshad², Muhammad Asad³, Amanullahkhan Pathan⁴, Amjad Ammar Qureshi⁵, Nadim Imtiyaz Shaikh⁶, Muhammad Shahid⁷

¹ *Electronic Engineering Department, Quaid-e-Awam University of Engineering, Science and Technology, Nawabshah, PAKISTAN.*

² *Department of Electrical Power Engineering, Faculty of Electrical and Electronic Engineering, University Tun Hussein Onn Malaysia, Johor, MALAYSIA.*

³ *Commissioning Services Division-Central, National Grid, SAUDIA ARABIA.*

⁴ *Department of Power Transmission and Distribution, Larsen and Toubro, SAUDIA ARABIA.*

⁵ *Department of Assets and Engineering Management, Trafigura Nyrstar, AUSTRALIA.*

⁶ *Department of Power Transmission and Distribution (IC), Larsen and Toubro, SAUDIA ARABIA.*

⁷ *Department of Protection & Automation Engineering, Siemens Ltd, SAUDI ARABIA.*

**Corresponding Author (Tel: +92-3322690991, erumasad79 @ gmail.com)*

Paper ID: 12A2P

Volume 12 Issue 2

Received 15 September 2020

Received in revised form 24 November 2020

Accepted 10 December 2020

Available online 14 December 2020

Keywords:

Microgrid (MG); Voltage & Frequency (V&F); H-infinity (H^∞); Low Pass filter (LPF); Distributed Grid (DG); Droop control.

Abstract

The future of the power system is definitely depending on the micro grid (MG) system which includes the Distribution Generators utilizing the Renewable energy Resources (RERs) and Storage. In this paper, an H^∞ VF control strategy is presented for a parallel islanded AC microgrid system. The control strategy restored desired results accurately by removing errors of voltage and frequency (V&F) at a nominal value without using the secondary controller in addition to improving the active power and reactive power accuracy by using the proposed robust droop control. The proposed control scheme has been tested through MATLAB/Simulink under different load conditions. The comparison proves the effectiveness of the proposed controller which improves the desired results in frequency and voltage perspective. The proposed controller is reliable and stable than a conventional and secondary controller.

Disciplinary: Electrical Engineering and Technology.

©2021 INT TRANS J ENG MANAG SCI TECH.

Cite This Article:

Pathan, E., Khan, M. H., Arshad, H., Asad, M., Pathan, A. K., Qureshi, A. A., Shaikh, N. I. (2021). H-Infinity VF Controller-Based Three-Phase Voltage Source Parallel Autonomous Grid. *International Transaction Journal of Engineering, Management, & Applied Sciences & Technologies*, 12(3), 12A2P, 1-13. <http://TUENGR.COM/V12/12A2P.pdf> DOI: 10.14456/ITJEMAST.2021.37

1 Introduction

Distributed Generation (DG) units are combined to develop a microgrid (MG) system which is the future of the modern power system [1] MG system is addressing the issues of the traditional power system successfully. The issues like reliability, stability, transmission losses, cost, environmental, and power quality are the reasons behind the development of the MG system [2]. MG system still has a lot of issues that need to be resolve for practical implementation especially in terms of control. Reactive power flow, voltage, and frequency stability in the operating conditions that are on-grid and off-grid must be in an acceptable range to ensure a smooth MG operation [3]. Moreover, a proper scheme that can handle V&F errors of the microgrid system for establishing an autonomous MG control is essential.

For the off-grid (islanded) mode of operation, there are several methods to control the MG system for example the Master-slave control [4], the multi-agent control system [5], and the multi-agent system is communication-based control that needs a communication link for control. On the other hand droop control is a communication less control technique [6]. In the islanded mode of operation, the droop control technique facilitates the decentralization operation of MGs and voltage and frequency. Active power frequency (P/f) and reactive power voltage (Q/v) droop control mechanisms are simple to implement and retains the voltage, frequency in a specific required range, especially in islanded MGs [7]. The Droop control with a virtual impedance loop can be implemented to handle frequency, voltage, and power-sharing issues [8]. In the literature, many researchers used modified droop control to get their required control. The droop coefficients are adjusted in such a way that modifies the conventional droop control and used for error elimination of voltage and frequency [9]

H-infinity (H^∞) control mechanism is implemented with the droop control to mitigate the voltage and frequency errors. H^∞ control is considered to be a multi-objective solver to handle the various control tasks [10]. In [11], H^∞ is implemented with droop control. The voltage and frequency errors under various load conditions were tested and ratified by using the H^∞ control. Moreover, the proposed controller scheme tested for unbalanced and nonlinear loads too [12]. H^∞ controller by utilizing linear matrix inequalities techniques for islanded voltage source inverter-based MG implemented in [13]. The technique is applied to the primary level and primary frequency is controlled as well as the system stability is tested using the μ synthesis. Particle swarm optimization (PSO) technique for the solution of frequency deviations presented in [14] and power-sharing accuracy in [15, 16]. Implementing the PSO technique along with the H^∞ control ensures the power-sharing accuracy with the system stability. Nevertheless, the control technique shows good simulation results against voltage and current errors and reduced THD.

In [12–17], mostly the H^∞ controller is used to handle the only one parameter that may be the frequency, voltage, current or power-sharing accuracy. This paper presents a robust and simple approach for an inverter-based islanded MG system. The control is based on the H^∞ control technique. Droop controller scheme utilized with H^∞ control that significantly enhanced VF results

as compared to conventional ones. Moreover, the proposed control technique can handle the power quality by implementing an H^∞ controller to the LCL filter and also at current or voltage loops. These are the two ways where the H^∞ controller is used to enhance power quality issues in Islanded MG system. The proposed control is repetitive as well as adaptive. Voltage and current tracking are done through the internal model principle and load changing conditions are responded to accordingly to mitigate the voltage, frequency, and power-sharing accuracy errors. The proposed control scheme is tested to multi DG based MG system with different balanced and unbalanced loads. Conventional droop control is modified and implemented to get the improved power quality. Moreover, the stability of the MG system is tested by root locus and step response. The Controller has the ability to regain its initial position after fault clearance.

2 Proposed Control H Based Method

In the microgrid control system besides other control issues the droop control mechanism facing some core concerns related to abrupt load change response because of these deficiencies the droop control cannot be helpful to mitigate the frequency and voltage errors at the load varying

The proposed control scheme is designed to get rid of the issues caused by droop control. Moreover, the control scheme is capable to get its steady-state conditions. Nevertheless, the proposed control scheme is also capable to mitigate mismatching among generation and load in off-grid operation and voltage frequency errors are successfully removed.

The H controller is a very useful controller, especially in MG control techniques. The proposed controller guarantees the stability of the MG system and can handle uncertain situations in load. Voltage and frequency errors are removed by the proposed H controller by utilizing the linear feedback configuration.

In the given feedback configuration u , w , y , and z represent the control input, error, output measurement, and controlled output respectively. The H controller is implemented for determining the closed-loop transfer function of w and z . For the design of the H controller, disturbances are handled in such a way that the input y and output u are designed for the controller C .

In Figure 1, ε & μ w delay time $e^{(-T_d)}$ are given to assurance of the conditions to keep it stable. These parameters are the weighting parameters. The delay time T_d with ω_c cut-off frequency of LPF, is calculated as

$$W(s) = \frac{W_c}{S + W_c} \quad (1),$$

$$T_d = T - \frac{1}{\omega_c} \quad (2).$$

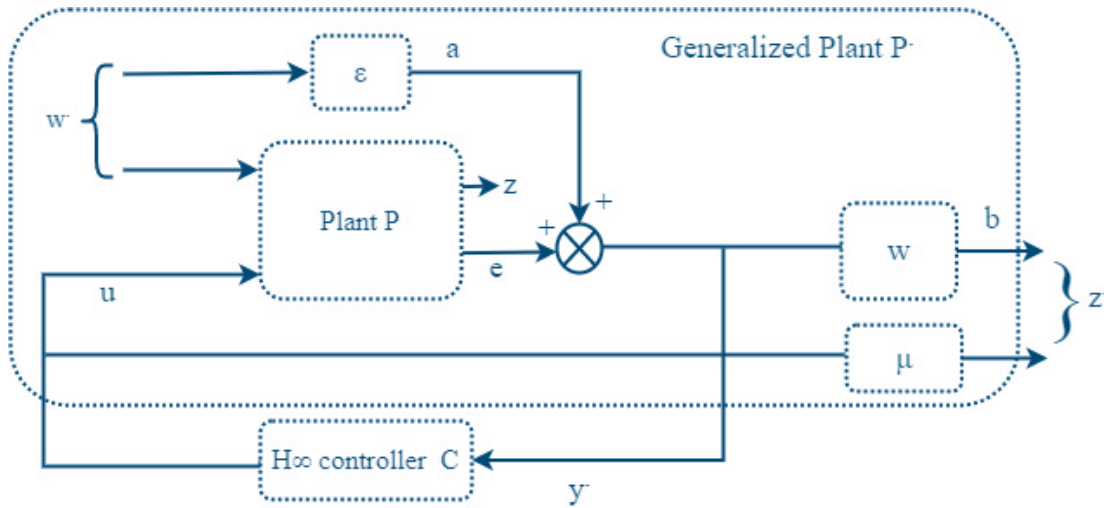


Figure 1: Formulation of the proposed controller

The H ∞ controller's voltage and current loops [18] having ε and weighted parameters, the closed-loop system is given as;

$$\begin{aligned}
 \begin{bmatrix} \dot{z} \\ y \end{bmatrix} &= P \begin{bmatrix} w \\ u \end{bmatrix}, u = CYz \\
 W &= \begin{bmatrix} \varepsilon A_w & B_w \\ \varepsilon C_w & D_w \end{bmatrix} \begin{bmatrix} \dot{z} \\ z \end{bmatrix} = \begin{bmatrix} \varepsilon - w_{c1} & w_{c1} \\ \varepsilon & 1 \end{bmatrix} \begin{bmatrix} \dot{z} \\ z \end{bmatrix}
 \end{aligned} \tag{3}$$

where P is extended plant. From [14]

$$\begin{aligned}
 y &= e + \varepsilon v \\
 &= \varepsilon v + \begin{bmatrix} \varepsilon A_{inverter} & B_{inverter1} & B_{inverter2} \\ \varepsilon C_{inverter} & D_{inverter1} & D_{inverter2} \end{bmatrix} \begin{bmatrix} \dot{v} \\ v \\ u \end{bmatrix} \\
 &= \begin{bmatrix} \varepsilon A_{inverter} & 0 & B_{inverter1} & B_{inverter2} \\ \varepsilon C_{inverter} & \varepsilon & D_{inverter1} & D_{inverter2} \end{bmatrix} \begin{bmatrix} \dot{v} \\ v \\ \varepsilon w \\ \varepsilon u \end{bmatrix}
 \end{aligned} \tag{4}$$

$$\begin{aligned}
 Z_1 &= W(e + \varepsilon v) \\
 &= \begin{bmatrix} \varepsilon A_{inverter} & 0 & 0 & B_{inverter1} & B_{inverter2} \\ \varepsilon B_w C_{inverter} & A_w & B_w \varepsilon & B_w D_{inverter1} & B_w D_{inverter2} \\ \varepsilon & 0 & C_w & 0 & 0 \end{bmatrix} \begin{bmatrix} \dot{v} \\ v \\ \varepsilon w \\ \varepsilon u \end{bmatrix}
 \end{aligned} \tag{5}$$

$$Z_2 = m u \tag{6}$$

Combining the above equations, we get

$$P = \left[\begin{array}{cc|cc|c} \dot{e} & A_{inverter} & 0 & 0 & B_{inverter1} & B_{inverter2} \\ \hat{e} & B_w C_{inverter} & A_w & B_w e & B_w D_{inverter1} & B_w D_{inverter1} \\ \hat{e} & C_w C_{inverter} & C_w & D_w e & D_w D_{inverter1} & D_w D_{inverter2} \\ \hat{e} & 0 & 0 & 0 & 0 & m \\ \hat{e} & C_{inver} & 0 & e & D_{inver1} & D_{inver2} \end{array} \right] \dot{u} \quad (7).$$

The small-signal model can be computed as

$$C = \frac{\dot{e} A_c}{\hat{e} C_c} \left[\begin{array}{cc} B_{c1} & B_{c2} \\ D_{c1} & D_{c2} \end{array} \right] \dot{u} \quad (8),$$

$$[x_c] = A_c [x_c] + B_{c1} [v_{ref}] + B_{c2} [i_{idq} \quad v_{odq} \quad i_{odq}]^T \quad (9),$$

$$[y_c] = C_c [x_c] + D_{c1} [v_{ref}] + D_{c2} [i_{idq} \quad v_{odq} \quad i_{odq}]^T \quad (10),$$

where

$$A_c = \begin{bmatrix} \dot{e} \omega_{ref} - m_p & 0 & 0 & 0 & 0 & 0 \\ \hat{e} 0 - \omega_c & 0 & 0 & 0 & 0 & 0 \\ \hat{e} 0 & 0 & -\omega_c & 0 & 0 & 0 \\ \hat{e} 0 & 0 & -n_q & 0 & 0 & 0 \\ \hat{e} 0 & 0 & 0 & 0 & 0 & 0 \\ \hat{e} 0 & 0 & -K_{pv} n_q & K_{iv} & o & o \\ \hat{e} 0 & 0 & 0 & 0 & K_{iv} & o \end{bmatrix}, B_{c1} = \begin{bmatrix} \dot{e} 0 \\ \hat{e} 0 \\ \hat{e} 0 \\ \hat{e} 1 \\ \hat{e} 0 \\ \hat{e} K_{pv} \\ \hat{e} 0 \end{bmatrix} \dot{u}$$

$$x_c = [d_i \quad P_i \quad Q_i \quad j_{dq} \quad g_{dq}]^T$$

$$[y_c] = [w \quad v_{odq}^* \quad i_{ldq}^* \quad v_{idq}^*]^T$$

$$D_{c1} = [0 \quad 1 \quad 0 \quad K_{pv} \quad o \quad K_{pc} \quad K_{pv} \quad 0]^T$$

$$B_{c2} = \begin{bmatrix} \dot{e} 0 & 0 & 0 & 0 & 0 & 0 \\ \hat{e} 0 & 0 & 1/2 \omega_c i_{od} & 1/2 \omega_c i_{oq} & 1/2 \omega_c i_{od} & 1/2 \omega_c i_{oq} \\ \hat{e} 0 & 0 & 1/2 \omega_c i_{oq} & -1/2 \omega_c i_{od} & -1/2 \omega_c i_{oq} & 1/2 \omega_c i_{od} \\ \hat{e} 0 & 0 & -1 & 0 & 0 & 0 \\ \hat{e} 0 & 0 & 0 & -1 & 0 & 0 \\ \hat{e} 1 & 0 & -K_{pv} & -\omega_c C_f & F & o \\ \hat{e} 0 & -1 & -\omega & -K_{pv} & 0 & F \end{bmatrix} \dot{u}$$

$$c_c = \begin{bmatrix} \hat{e} W_{ref} & -m_p & 0 & 0 & 0 & 0 & 0 & \hat{u} \\ \hat{e} 0 & 0 & -n_q & 0 & 0 & 0 & 0 & \hat{u} \\ \hat{e} 0 & 0 & 0 & 0 & 0 & 0 & 0 & \hat{u} \\ \hat{e} 0 & 0 & -n_q K_{pv} & K_{iv} & 0 & 0 & 0 & \hat{u} \\ \hat{e} 0 & 0 & 0 & 0 & K_{iv} & 0 & 0 & \hat{u} \\ \hat{e} 0 & 0 & 0 & K_{pc} K_{iv} & 0 & K_{ic} & 0 & \hat{u} \\ \hat{e} 0 & 0 & 0 & 0 & K_{pc} K_{iv} & 0 & K_{ic} & \hat{u} \end{bmatrix}$$

The calculation of the TF from a to b is given below provided

$$D_{c2} = \begin{bmatrix} \hat{e} W_{ref} & 0 & 0 & 0 & 0 & 0 & 0 & \hat{u} \\ \hat{e} 0 & 0 & 0 & 0 & 0 & 0 & 0 & \hat{u} \\ \hat{e} 0 & 0 & 0 & 0 & 0 & 0 & 0 & \hat{u} \\ \hat{e} 0 & 0 & -K_{pv} & -W_n C_f & F & 0 & 0 & \hat{u} \\ \hat{e} 0 & 0 & -W_n L_f & -K_{pv} & 0 & F & 0 & \hat{u} \\ \hat{e} -K_{pc} & -W_n L_f & -K_{pc} K_{pv} & -K_{pc} W_n C_f & K_{pc} F & 0 & 0 & \hat{u} \\ \hat{e} -W_n L_f & -K_{pc} & -K_{pc} W_n C_f & -K_{pc} K_{pv} & 0 & K_{pc} F & 0 & \hat{u} \end{bmatrix}$$

that $\omega = 0$.

$$T_{ba} = \frac{\begin{bmatrix} \hat{e} A_{inverter} + B_{inverter2} D_c C_{inverter} & B_{inverter2} C_c & B_{inverter2} D_c C_w \\ \hat{e} B_c C_{inverter} & A_c & B_c C_w \\ \hat{e} 0 & 0 & A_w \\ \hat{e} C_{inverter} & 0 & C_w \end{bmatrix}}{\begin{bmatrix} 0 \\ 0 \\ B_w \\ 0 \end{bmatrix}} \begin{bmatrix} \hat{u} \\ \hat{u} \\ \hat{u} \\ \hat{u} \end{bmatrix} \quad (11)$$

When controller C is obtained, the next step is to verify the controller's stability that can be validated by inspection $\|T_{ba}\|_{\infty}$.

3 Result and Discussion

The proposed control scheme is tested under the MATLAB/Simulink as per the control strategy shown in Figure 2, and system load parameters are given in Table 1 model with two parallel DG-based microgrids is built using MATLAB/Simulink. Sudden load switching time and load ratings are given in Table. During the switching of loads, the time domain response of power-sharing, the total power of microgrid, voltage and frequency are analysed for effectiveness confirmation. It is proved from simulation testing that robust H_{∞} decentralized power-sharing controller over the secondary hierarchical controller and the conventional decentralized primary power-sharing controller.

Table 1: Switching time of sudden load and power ratings of low to medium to high to medium loads.

| Parallel inverters | Loads | Rating | Switch On-OFF time |
|-----------------------------------|------------------|--------|--------------------|
| DG ₁ & DG ₂ | P _{L 1} | 500 W | 0–1 s |
| | P _{L 2} | 1000 W | 1–2 s |
| | P _{L 3} | 1600 W | 2–3 s |
| | P _{L 4} | 700 W | 3–4 s |

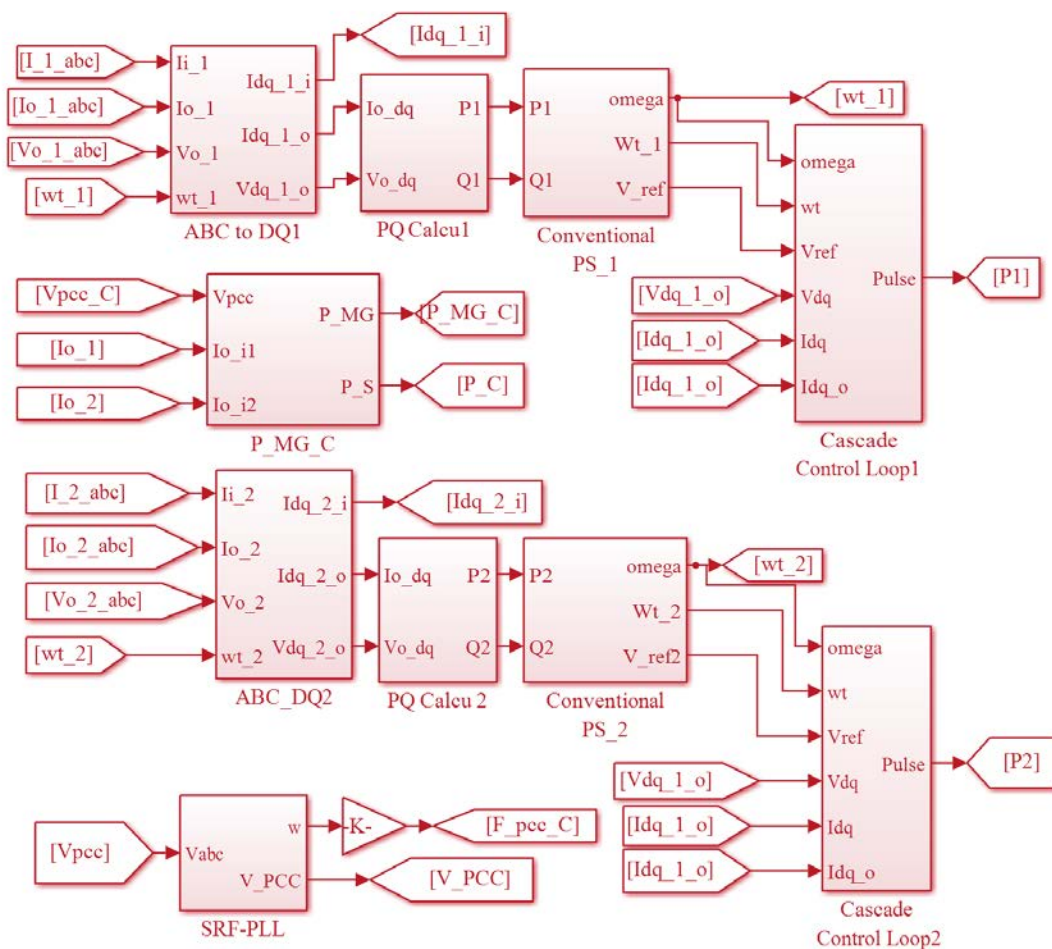
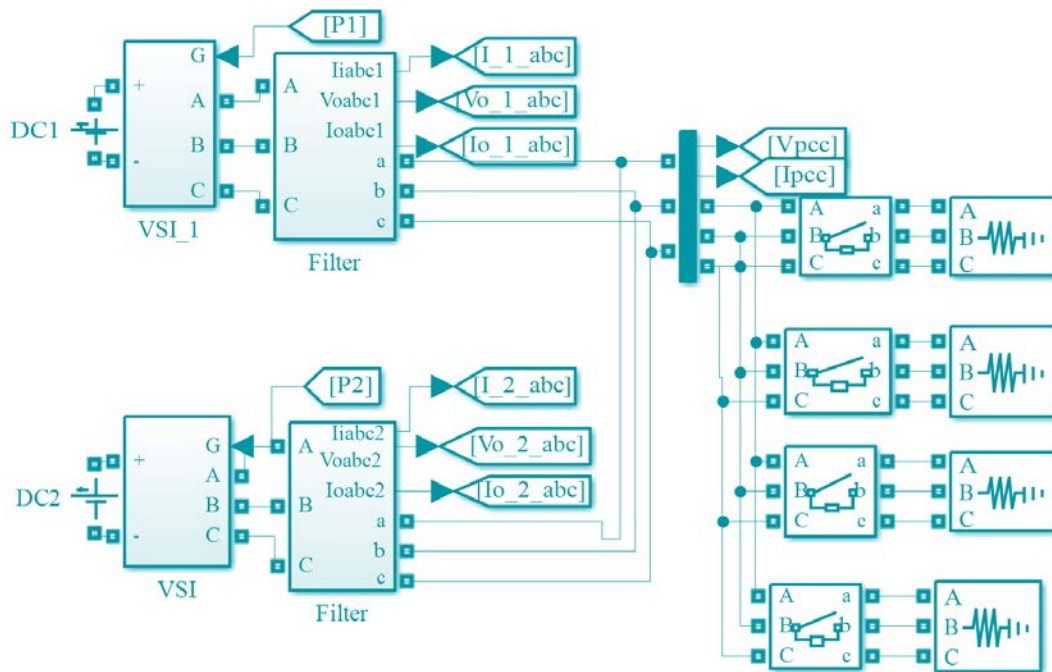


Figure 2: A simulation model for the proposed controller

The current and voltage analysis at PCC of parallel DGs in islanded mode when the DGs are connected with low, medium, high, and then medium loads at 0-1 s, 1-2 s, 2-3 s, and 3-4 s, respectively, Figure 3, 4 and 5 illustrate the voltage response.

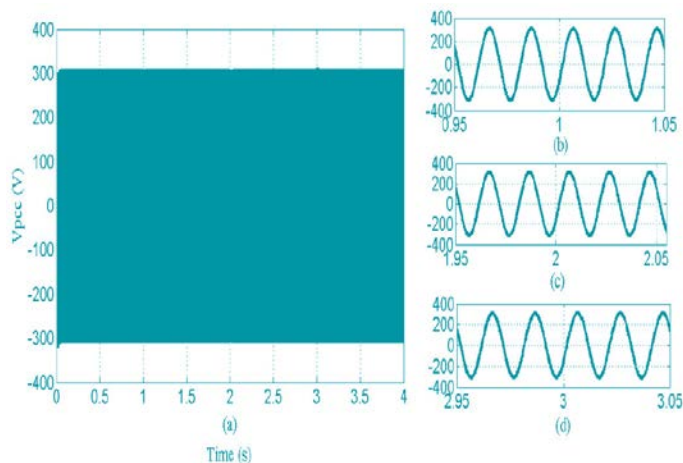


Figure 3: H^∞ -based DGs' voltage response at PCC (a), zoomed response from LM load change (b), zoomed response from MH load change (c), and zoomed response from HM load change (d)

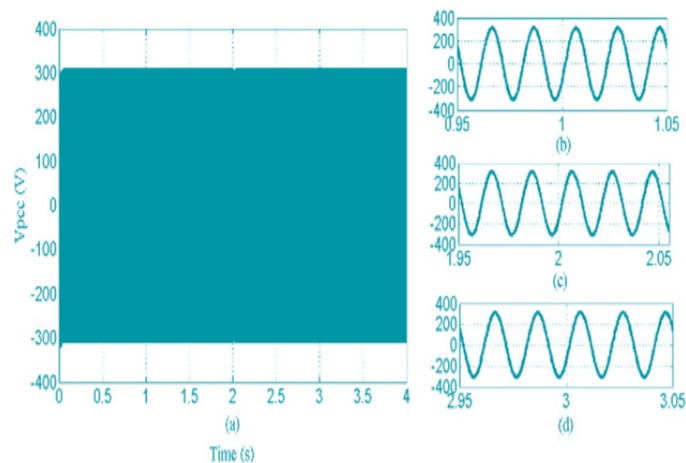


Figure 4: Secondary-based DGs' voltage response at PCC (a), zoomed response from LM load change (b), zoomed response from MH load change (c), and zoomed response from HM load change (d)

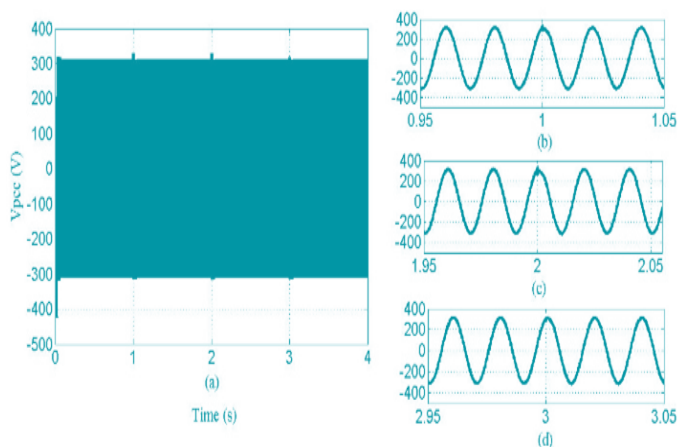


Figure 5: Conventional-based DGs' voltage response at PCC (a), zoomed response from LM load change (b), zoomed response from MH load change (c), and zoomed response from HM load change (d)

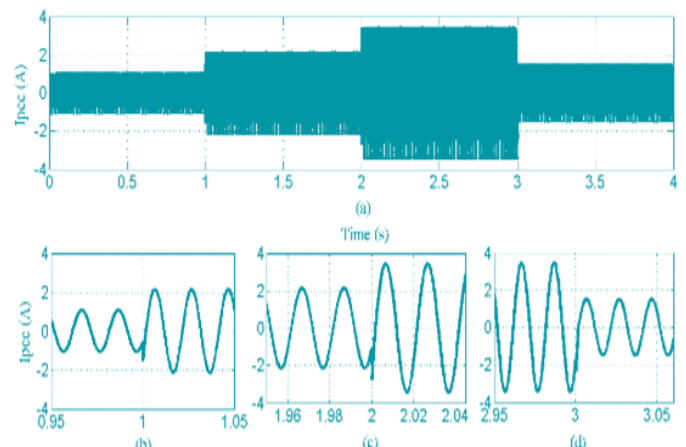


Figure 6: H^∞ -based DGs current response at PCC (a), zoomed Response from LM load change (b), zoomed response from MH load change (c), and zoomed response from HM load change (d)

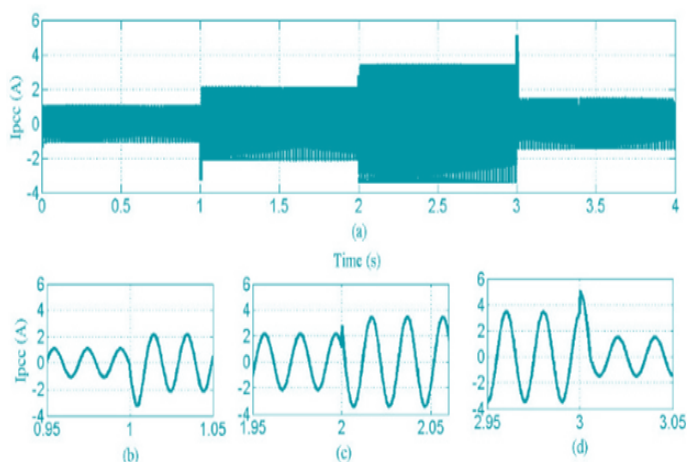


Figure 7: Secondary-based DGs' current response at PCC (a), zoomed response from LM load change (b), zoomed response from MH load change (c), and zoomed response from HM load change (d)

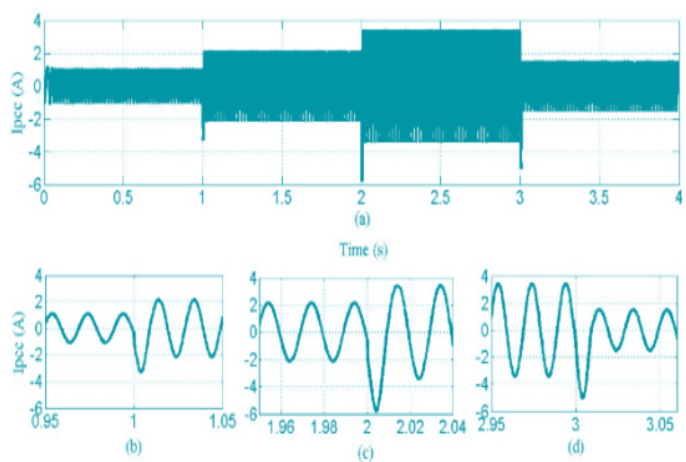


Figure 8: Conventional-based DGs current response at PCC (a), zoomed response from LM load change (b), zoomed response from MH load change (c), and zoomed response from HM load change (d).

Figures 6, 7, and 8 showing the current response according to the H^∞ -based DGs, the secondary-based DGs, and the conventional-based DGs at the point of common coupling during different load changes. The voltage response is smooth in all cases with just a slight spike in the conventional controller during load variations. It clearly shows that smooth transient current is flowing when the load is suddenly changed and that the parallel islanded system behavior is stable.

Figure 9 shows the active sharing power and Figure 10 for total microgrid power with two identical DGs when the loads are connected from low to medium to high to medium. The total simulation time is 4 s, and the loads are suddenly changed from low to medium at 1–2 s, from medium to high at 2–3 s, and from high to medium at 3–4 s.

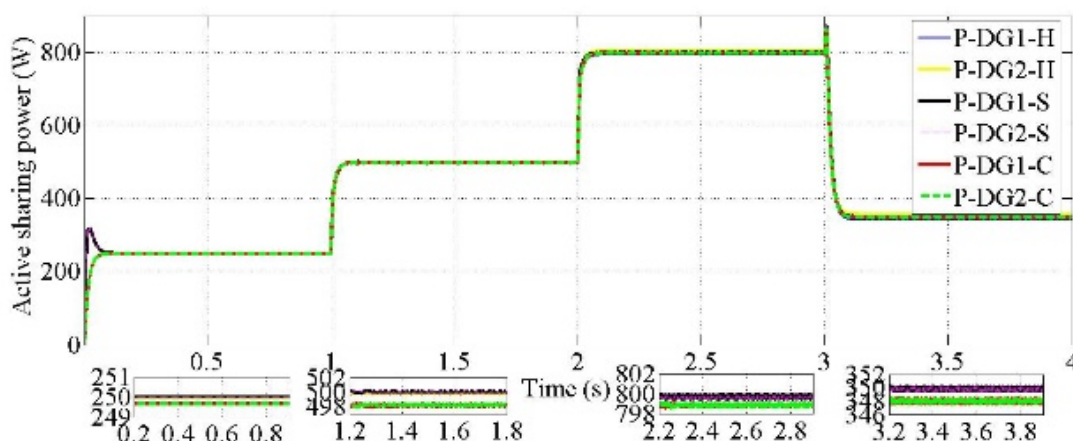


Figure. 9: Active sharing power time domain response for low-medium-high-medium load change ($H = H^\infty$, $S =$ secondary, $C =$ conventional primary).

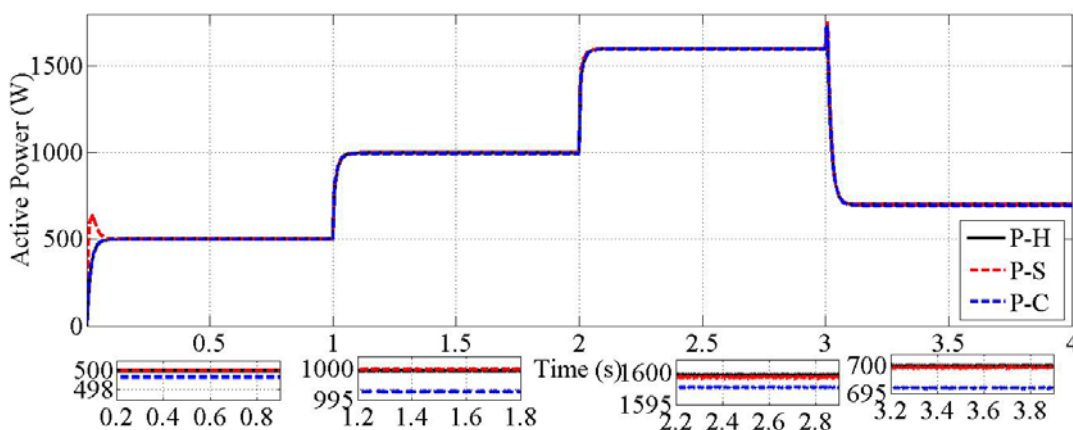


Figure. 10: Active power time domain response for low-medium-high-medium load change ($H = H^\infty$, $S =$ secondary, $C =$ conventional control).

Figures 11 and 12 illustrate the signal analysis, based on the transient behavior of frequency and voltage of AC microgrid at PCC, respectively. The step response of conventional, existing secondary, and proposed robust H^∞ controller is illustrated in Figure 11 (a). Figure 11 (b) indicates that the existing secondary controller has a slower rise time of 0.3 s than the proposed robust H^∞

controller rise time is 0.053 s during the first load condition. As suddenly load is changed during 1-2 s, the rise time is 1.001 s and high peak in the conventional system. the frequency deviates more and is not retained back to its nominal value. Whereas the existing secondary controller has a slower rise time of 1.2 s because of the processing delay with a high peak and restored the frequency to the nominal value. the response under the proposed robust controller is illustrated in a fast manner with 1.02 s rise time and good tracking performance with 4% overshoot. when the load is suddenly changed from low to medium as in Figure 11 (c) or from medium to high as in Figure 11 (d), as well as from high to medium as in Figure 11 (e), in all conditions the frequency slightly deviates but it is again retained back to nominal frequency quickly. Whereas, in the conventional system, the frequency deviates more and is not retained back to its nominal value during load changes. Thus, the proposed robust distributed H^∞ active power and frequency controller works properly and maintains the nominal frequency level without applying any communication link or secondary hierarchical controller.

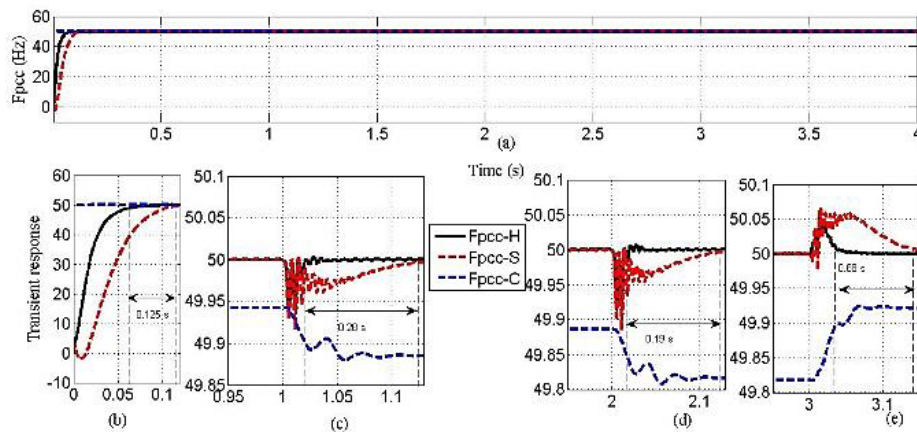


Figure. 11: Frequency time domain response for low-medium-high-medium load change (a), TR at PCC (b), TR of LM load change (c), TR of MH load change (d), and TR of HM load change (e) (H = H^∞ , S = secondary, C = conventional).

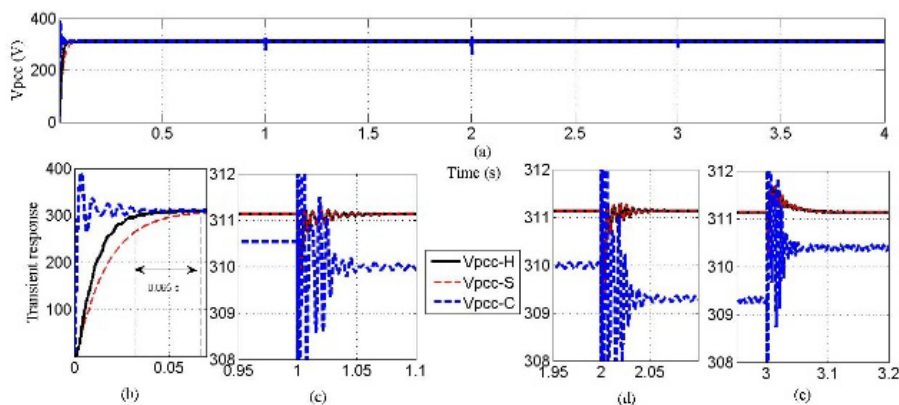


Figure. 12: Voltage time-domain response for LMHM load change (a), the transient response at PCC (b), TR of LM load change (c), TR of MH load change (d), and TR of HM load change (e) (H = H^∞ , S = secondary, C = conventional).

Moreover, Figure 12 (a) depicts the transient behaviour of voltage at PCC. The proposed H^∞ reactive power and voltage controller loop show its effectiveness. Figure 12 (b) indicates that the transient VPCC response is slower in the secondary controller because of process delay, whereas the proposed robust H^∞ controller has a faster transient response. The system voltage is at the nominal value at 0-1 s during the first low load. The load is changed from low to medium level as in Figure 12 (c), and the voltage slightly deviates and is restored to its nominal value at 1-2 s.

The same system is tested with medium-to-high load change and vice versa during 2-3 s as in Figure 12 (d) and 3-4 s as in Figure 12 (e), respectively, and the microgrid voltage slightly deviates but again back to the nominal voltage level by using the secondary hierarchical communication-based control and the proposed robust distributed H^∞ control technique. Meanwhile, the system voltage deviates more after the load is changed in the conventional power-sharing technique. Thus, the proposed robust H^∞ reactive power and voltage controller improves the accuracy of the desired voltage without applying any communication link or secondary hierarchical control loop. It increased the efficiency of the controller response by 95% for reference value tracking, good tracking response by reducing the 4% of overshoot.

4 Conclusion

In this paper, the robust H^∞ VF controller is used to resolve the power-sharing issues without compromising the power quality of the system. Improve the power-sharing of active and reactive power in parallel DGs. the proposed control scheme is tested with different load conditions by using the MATLAB Simulink environment proposed control scheme is applied to the microgrid with two parallel-connected inverters having different loads. The proposed controller is adjusted the system VF as well as improving the system stability and sharing of active and reactive power quality. Moreover, the proposed system is more effective than the conventional and existing secondary controller by designing the proper weighted function and H^∞ controller parameters.

5 Availability of Data And Material

Data can be made available by contacting the corresponding authors.

6 References

- [1] A. Hirsch, Y. Parag, and J. Guerrero, "Microgrids: A review of technologies, key drivers, and outstanding issues," *Renew. Sustain. Energy Rev.*, vol. 90, September 2017, pp. 402-411, 2018.
- [2] F. H. Gandoman *et al.*, "Review of FACTS technologies and applications for power quality in smart grids with renewable energy systems," *Renew. Sustain. Energy Rev.*, vol. 82, pp. 502-514, 2018.
- [3] Z. Abousserhane, A. Abbou, L. Id-Khajine, and N. E. Zakzouk, "Power Flow Control of PV System Featuring On-Grid and Off-Grid Modes," *Proc. 2019 7th Int. Renew. Sustain. Energy Conf. IRSEC*, 2019.

- [4] A. D. Bintoudi *et al.*, “An improved decentralised coordinated control scheme for microgrids with AC-coupled units,” *2018 Int. Conf. Smart Energy Syst. Technol. SEST 2018 - Proc.*, pp. 2-7, 2018.
- [5] R. Garduno-Ramirez and M. Borunda, “An intelligent multi-agent-based improved approach for conventional and renewable power generation operation and control,” *J. Renew. Sustain. Energy*, 9(1), 2017.
- [6] Z. Peng *et al.*, “Droop control strategy incorporating coupling compensation and virtual impedance for microgrid application,” *IEEE Trans. Energy Convers.*, vol. 34, no. 1, pp. 277-291, 2019.
- [7] N. M. Dehkordi, N. Sadati, and M. Hamzeh, “Robust tuning of transient droop gains based on Kharitonov’s stability theorem in droop controlled microgrids,” *IET Gener. Transm. Distrib.*, vol. 12, no. 14, pp. 3495-3501, 2018.
- [8] E. Planas, A. Gil-De-Muro, J. Andreu, I. Kortabarria, and I. Martínez De Alegría, “General aspects, hierarchical controls and droop methods in microgrids: A review,” *Renew. Sustain. Energy Rev.*, vol. 17, pp. 147-159, 2013.
- [9] A. Sheela, S. Vijayachitra, and S. Revathi, “H-infinity controller for frequency and voltage regulation in grid-connected and islanded microgrid,” *IEEJ Trans. Electr. Electron. Eng.*, vol. 10, no. 5, pp. 503-511, 2015.
- [10] H. A. and M. A. E.Pathan, A.A.Bakar, S.A. Zulkifi, M.H.Khan., “A Robust Frequency Controller based on Linear Matrix Inequality for a Parallel Islanded Microgrid,” *Eng. Technol. Appl. Sci. Res.*, vol. 10, no. 5, pp. 6264-6269, 2020.
- [11] H. A. T. Hamid Reza Baghaee, Mojtaba Mirsalim, Gevork B. Gharehpetian, “A generalized descriptor-system robust H-infinity control of autonomous microgrids to improve small and large signal stability considering communication delays and load nonlinearities,” *International Journal of Electrical Power & Energy Systems*, 1 pp. 1-20, 2017.
- [12] Q. L. Lam, A. I. Bratcu, and D. Riu, “Robustness Analysis of Primary Frequency H_{∞} Control in Stand-alone Microgrids with Storage Units,” *IFAC-PapersOnLine*, vol. 49, no. 27, pp. 123-128, 2016.
- [13] J. Zhao and C. Wang, “Frequency stability of microgrids based on H_{∞} methods,” *Chinese Control Conf. CCC*, vol. 2016, pp. 10079-10084, 2016.
- [14] B. E. Sedhom, A. Y. Hatata, M. M. El-Saadawi, and E. H. E. Abd-Raboh, “Robust adaptive H-infinity based controller for islanded microgrid supplying non-linear and unbalanced loads,” *IET Smart Grid*, vol. 2, no. 3, pp. 420-435, 2019.
- [15] B. E. Sedhom, M. M. El-Saadawi, A. Y. Hatata, and E. H. E. Abd-Raboh, “H-infinity versus model predictive control methods for seamless transition between islanded- A nd grid-connected modes of microgrids,” *IET Renew. Power Gener.*, vol. 14, no. 5, pp. 856-870, 2020.
- [16] S. Choudhury, L. Mohapatra, and P. K. Rout, “A comprehensive review on modeling, control, protection and future prospects of Microgrid,” *Int. Conf. Electr. Electron. Signals, Commun. Optim. EESCO 2015*, January 2015.
- [17] T. Hornik and Q. C. Zhong, “A current-control strategy for voltage-source inverters in microgrids based on H_{∞} and Repetitive Control,” *IEEE Trans. Power Electron.*, vol. 26, no. 3, pp. 943-952, 2011.

- [18] E. Pathan, S. Zulkifli, U. Tayab, and R. Jackson, "Small Signal Modeling of Inverter-based Grid-Connected Microgrid to Determine the Zero-Pole Drift Control with Dynamic Power Sharing Controller," *Eng. Technol. Appl. Sci. Res.*, vol. 9, no. 1, pp. 3790-3795, 2019.
-



Dr. Erum Pathan is an Assistant Professor at the Department of Electrical Power Engineering, Faculty of Electronic Engineering of Quaid-E Awam University of Engineering, Science and Technology Nawabshah, Sindh, Pakistan. She received a B.E in Electronic Engineering, an M.E degree in Telecommunication & Control from Mehran University of Engineering and Technology, Jamshoro, Pakistan and a PhD degree in Electrical Engineering from University Tun Hussein Onn, Malaysia. Her research areas include robust control theory in smart grid application, parallel inverter and Smart grid Control. She is also a member of Pakistan Engineering Council.



Mubashir Hayat Khan a Lecturer at the Department of Electrical Engineering, Faculty of Engineering and Technology, University of Poonch Rawalakot (UPR). He obtained a B.Sc. (Hons.) and MS Degrees from Mirpur University of Science & Technology, AJ&K Pakistan. He is a PhD research scholar at the University Tun Hussein Onn Malaysia, in the Faculty of Electrical Engineering. His research area is Inverter-based Smart grid Control.



Haider Arshad is a postgraduate research student in UTHM Malaysia. He obtained his BSc Electrical Engineering degree from University of Poonch. His research interests include Smart Grids, Electric Vehicle Control and Power-Sharing Applications like V2G and G2V, Power Flow Control and Grid Connected Inverters.



Dr. Muhammad Asad Shaikh received a B.E in Electrical Power Engineering from QUEST, Pakistan & a PhD degree in Electrical Engineering from Bakerville University. Also, he received a B.A degree, a DIT, Internship certificates in various power sector companies and he has received technical, management and 5-Star Safety training. He is an active member of Saudi & Pakistan Engineering Council. He has 15 years' international Experience and Commissioned 26 Projects including Static VAR Compensation, Fixed Series Compensation and 380/132/13.8KV Power Substation including BSP, he has sound technical experience in the field of Substation Automation System, Control & SCADA Engineering (IEC61850, IEC60870-5-101/104), Project Management & Execution, Substation Testing and Commissioning, Power System Planning and Operation, Power System Fault Investigation & Reporting.



Amanullahkhan Pathan received the B.E in Electrical Power Engineering from Veer Narmad South Gujarat University. Additionally, he acquired PMP certification in 2020. He has great skills in Strategic Planning, Project Planning & Management, Process Improvement, Statutory Compliance, Resource Planning & Budgeting, Project Management, Cost & Control, and Quality Control Management. He has 15 years' international Experience in Power sector of End-To-End Experience in Managing, Executing, Project Planning, Coordination & Implementation from Scope Management to Activity Sequencing, Effort & Cost Estimation and Risk Analysis to Operation Management in Line with Guidelines.



Amjad Ammar Qureshi is a Chartered Professional Engineer, a recognized global technical authority in Electrical, Instrumentation, Integrated Control Systems, IIOT based Automation Systems and Communication systems. Having delivered EPCC multibillion-dollar projects in Asia, Pacific and NA regions in the last 15 years, currently leading large scale Engineering Projects of Trafigura Nyrstar.



Nadim Imtiyaz Shaikh received a B.E in Electrical Power Engineering from Sarvajanik College of Engineering and Technology, Veer Narmad South Gujarat University, Surat. Additionally, he acquired PMP certification in 2020. He is a result-oriented Project Management Professional with 12 years of rich experience in Power Transmission and Distribution section, Project Executions & Maintenance experience in Utility companies. He focused & goal-oriented, adept at Creating & Formulating Strategies for Accelerated Growth, Hard Working with Unsurpassed Communication, Organized Presentation & Interpersonal Skills



Muhammad Shahid received a B.E in Electrical Power Engineering from Preston University, Pakistan. Also, he received a DIT certification. He has sound international experience in IEC61850 Substation Automation Engineering, SCADA Gateways IEC60870-5-101/104 Integration and, has commissioned 24 Projects.
